

# Enhanced antiproton production in Pb(160 AGeV)+Pb reactions: evidence for quark gluon matter?

M. Bleicher<sup>a,ξ</sup>, M. Belkacem<sup>b</sup>, S.A. Bass<sup>c</sup>, S. Soff<sup>d</sup>, H. Stöcker<sup>d</sup>

<sup>a</sup> *Nuclear Science Division, Lawrence Berkeley National Laboratory,  
Berkeley, CA 94720, USA*

<sup>b</sup> *School of Physics and Astronomy, University of Minnesota  
Minneapolis, MN 55455, USA*

<sup>c</sup> *National Superconducting Cyclotron Laboratory, Michigan State University  
East Lansing, MI 48824-1321, USA*

<sup>d</sup> *Institut für Theoretische Physik, Goethe-Universität,  
60054 Frankfurt am Main, Germany*

## Abstract

The centrality dependence of the antiproton per participant ratio is studied in Pb(160 AGeV)+Pb reactions. Antiproton production in collisions of heavy nuclei at the CERN/SPS seems considerably enhanced as compared to conventional hadronic physics, given by the antiproton production rates in  $pp$  and antiproton annihilation in  $\bar{p}p$  reactions. This enhancement is consistent with the observation of strong in-medium effects in other hadronic observables and may be an indication of partial restoration of chiral symmetry.

---

E-mail: bleicher@nta2.lbl.gov

<sup>ξ</sup> Feodor Lynen Fellow of the Alexander v. Humboldt Foundation

One of the goals of relativistic heavy-ion research is the exploration of the phase diagram of hot and dense nuclear matter [1,2]. Abundances and ratios of hadrons produced in these collisions have been suggested as possible signatures for exotic states and phase transitions occurring in the course of the reaction [3–5]. E.g. strangeness and antibaryon enhancement due to gluon fragmentation into  $q\bar{q}$  pairs [5]. Bulk properties like temperatures, entropies and chemical potentials of highly excited hadronic matter have been extracted from high energy heavy ion data assuming thermal and chemical equilibrium [2–8]. However, despite the recent announcement of circumstantial evidence for the formation of a quark gluon plasma (QGP) at the CERN Super-Proton-Synchrotron (SPS) [9], unambiguous signals of a phase transition into an equilibrated QGP state are still missing.

The variation of hadron ratios involving anti-baryons as a function of centrality has been proposed in [10] as a method to distinguish equilibrium from non-equilibrium scenarios. In models based on the assumption of thermal equilibrium (e.g. in thermal models or hydrodynamical models), the particle ratios are only sensitive to the temperature and chemical potentials at the freeze-out stage of the reaction. If the freeze-out criterion is universal, the ratios are completely insensitive to any dynamical quantities, e.g. the centrality of the reaction (in the extent one assumes the same baryon densities and temperatures at freeze-out). Microscopic transport theory, however, is not constrained by equilibrium assumptions. It is used to describe the full reaction dynamics, from the early non-equilibrium reaction stages up to hadronic freeze-out. On the other hand, the centrality dependence of hadron ratios provides a sensitive tool to probe the extent at which these ratios are described by a purely hadronic picture or by the invocation of more exotic pictures such as the formation of a QGP phase or partial chiral symmetry restoration. Thus, the centrality dependence of hadron ratios may provide a sensitive tool to probe the extent of the creation of a chemically equilibrated phase in collisions of heavy nuclei and distinguish different reaction scenarios. The recently published data by the NA49 collaboration on the ratios antiprotons per participant as a function of the number of participants [13] indicate a constant enhancement of anti-proton production as compared to  $pp$  results over the whole range of centralities

considered. The differences in the predicted centrality dependence among the discussed models as compared to data can be investigated to identify whether we observe an enhanced production of antimatter or a suppressed annihilation of antibaryons at CERN/SPS.

For our investigation we employ the Ultra-relativistic Quantum Molecular Dynamics model (UrQMD) [14]. UrQMD is a microscopic transport model with hadronic and constituent (di)quark degrees of freedom. Baryon-baryon, meson-baryon and meson-meson collisions lead to the formation and decay of resonances and color flux tubes. The produced particles, as well as the incoming particles, rescatter in the further evolution of the system.

Let us start by investigating the general features of antiproton production and annihilation in UrQMD: Antiprotons are produced via the decay of color flux tubes and in antiresonance decays (e.g.  $\overline{\Delta}^+ \rightarrow \overline{p} + \pi$ ). Since the collision dynamics in nucleus-nucleus is a convolution from high and low energy elementary collisions, it is important to verify that the energy dependence of the antiproton production is reasonable. Fig. 1 shows the multiplicity of antiprotons in inelastic  $pp$  interactions as a function of center of mass energy ( $\sqrt{s}$ ) compared to data. The UrQMD predictions, depicted as full circles, overestimate the experimental data (shown as full diamonds) by 50% in the SPS domain ( $\sqrt{s} = 20$  GeV). In line with data, the string model shows a strong increase of antiproton production with collision energies starting from a threshold of  $4m_{\text{proton}}$ . At higher energies, the production cross sections levels off at  $\overline{p}$  multiplicities of 0.1-0.2. However, the antiproton production will increase further at even higher energies, when the double antibaryon-baryon channels become populated.

In massive nuclear collisions, however, not only the production of antiprotons must be treated, but also antibaryon absorption can be important. In UrQMD the antiproton annihilation is modeled via the annihilation of quark-antiquark pair and the formation and subsequent decay of two color flux tubes with baryon number zero (for details see [14]). Fig. 2 confronts the UrQMD implementation of the antiproton-proton cross sections as a function of center of mass energy with experimental data [11]. The full line shows the total  $\overline{p}p$  cross section (data is shown as squares), the dotted line shows the elastic cross section (data as

triangles) and the dashed line depicts the annihilation cross section in UrQMD. In addition, the small inlay gives a detailed view of the cross sections from  $2m_{\text{proton}}$  to  $\sqrt{s} = 2$  GeV. This region is of special interest, since the antiproton absorption strongly increases towards low center of mass energies. Overall, a reasonable description of the antiproton-proton interactions over the energy range  $\sqrt{s} \leq 5$  GeV (most relevant for SPS) is obtained within the UrQMD model. Note that the sum of the annihilation cross section and the inelastic cross section is smaller than the total cross section. The difference  $\Delta\sigma = \sigma_{\text{total}} - \sigma_{\text{elastic}} - \sigma_{\text{annih.}}$  is assumed to be a pure inelastic cross section in  $\bar{p}p$  in analogy to  $pp$ .

Let us now turn towards the dynamics of nucleus-nucleus collisions at 160 AGeV. In addition to the  $pp$  case, meson-meson and meson-baryon interactions may also lead to the excitation of color flux tubes and their subsequent decay into baryon-antibaryon pairs. E.g. the channel  $\rho\rho \rightarrow \bar{B}B$  constitutes a new and unexplored production channel in AA collisions. On the other hand, the high baryon densities reached at central rapidities in nucleus-nucleus interactions can lead to an increased absorption of antiprotons. Fig. 3 shows the  $\bar{p}$ /participant<sup>1</sup>ratio for different centralities (given by the number of participating nucleons  $A_{\text{part}}$ ). Full squares show the standard UrQMD prediction of the  $\bar{p}/A_{\text{part}}$  ratio, while the data are depicted as full diamonds. A constant ratio over all centralities is observed both in experiment and calculation. In view of the large changes in the reaction dynamics when going from peripheral to central collisions the lack of  $A_{\text{part}}$  dependence in the  $\bar{p}/A_{\text{part}}$  ratio seems surprising. However, the UrQMD model calculations *underestimate* the data by a factor of 3! Considering the 50% overestimate in the elementary production channel (Fig. 1) this drastic deviation can only be explained by

1. strongly enhanced production,

---

<sup>1</sup>The number of participating nucleons in this paper is defined as:

$A_{\text{part}} = A_1 + A_2 - \Sigma(\text{Nucleons with } p_T \leq 270 \text{ MeV})$ . This prescription yields a reasonable parametrization of the experimental data on  $A_{\text{part}}$  as can be seen by comparison to Ref. [12].

2. strongly suppressed annihilation.

Within the UrQMD model, we are able to further investigate the cause of this behavior: since the elementary production and absorption cross sections are in line with the data, we expect one of the following scenarios to take place in AA collisions:

- A suppressed antiproton annihilation in dense matter, e.g. due to pion clouds which prevent annihilation. Such a screening effect has been speculated upon by [15].
- An enhanced production of antiprotons in AA, compared to  $pp$  extrapolations. This has been predicted by [5,16] as a signature of a QGP phase transition. It is interesting to note that studies by Koch et al. [5] and Ellis et al., [17] predict a factor 2.5 – 10 enhancement of the antibaryon production due to QGP formation. This  $\bar{p}$  source is also in line with recent measurements on the (anti-)hyperon enhancement in AA [18,19]. A remark here is in order: As stated above, the flat enhancement of  $\bar{p}/A_{\text{part}}$  as compared to  $pp$  results at all centralities is amazing. If the observed enhancement in the data is explained by the transition to the QGP, the same data indicate the formation of the QGP even in peripheral collisions (or in the smaller Sulphur-Sulphur system) where the formation of such a state seems less favourable due to the lower energy- and baryon-densities reached in these collisions.

To study the influence of these effects – and possibly distinguish between them – we alternatively incorporate the above mentioned effects into UrQMD and compare the results to the default scenario and the data.

First, Fig. 3 (open circles) shows the calculation with antibaryon annihilation turned off, as an extreme case of the screening assumption. This option leads to a reasonable description of the most central Pb+Pb interactions. However, the scaling of the  $\bar{p}/A_{\text{part}}$  ratio exhibits an increase of the ratio towards central collisions not in line with the NA49 data. Clearly, within the hadronic/string physics of UrQMD, antiproton production is enhanced in central collisions - annihilation is required to compensate this enhancement and obtain the flat

$\bar{p}/A_{\text{part}}$  ratio vs. centrality. We note also that the annihilation of anti-protons plays a counter-balancing role with anti-baryon production in secondary scattering (meson-baryon and meson-meson) to maintain the  $\bar{p}/A_{\text{part}}$  ratio constant versus  $A_{\text{part}}$ .

In order to test the deconfinement hypothesis, we perform a calculation with full antiproton absorption, but with an enhanced  $\bar{p}$  production cross section. Normally, one might think to enhance the cross-section smoothly from the  $pp$  cross-section at peripheral reactions to some large value for central collisions. In the present study, we chose a constant enhancement, adjusted to the most central collisions. This scenario, shown as open triangles in Fig. 3, leads to a flat  $\bar{p}/A_{\text{part}}$  ratio as function of centrality, in line with the data. This increase in antiproton production is due to an increase of the string tension by a factor of 2.6. This increase of the string tension results in an enhanced di-quark – anti-diquark production probability due to the Schwinger formula:

$$\gamma_{qq} = \frac{P(qq\bar{q}\bar{q})}{P(q\bar{q})} = \exp\left(-\frac{\pi(m_{qq}^2 - m_q^2)}{\kappa}\right). \quad (1)$$

leading to an increase of the diquark ‘suppression’ parameter  $\gamma_{qq}$  from 0.1 to 0.4. This spectacular increase of the string tension has recently been employed to reproduce the observed (anti-)hyperon enhancement at SPS energies [19]. It is consistent with the assumption of the onset of partial restoration of chiral symmetry which might lead to a decrease of the constituent quark masses towards current quark masses. The increased string tension can be alternatively motivated by the assumption of overlapping color flux tubes (“ropes”). Such superposition of the color electric fields can yield enhanced particle production [20,21]. In particular, heavy quark flavors and diquarks are dramatically enhanced [21–23].

---

<sup>2</sup>To be very specific: The light quark mass used in UrQMD is  $m_q = 0.223$  GeV and the diquark mass  $m_{qq} = 2m_q$ , the string tension is  $\kappa = 1$  GeV/fm =  $0.2$  GeV<sup>2</sup>, resulting in  $\gamma_{qq} = 0.095$ . These values provide a reasonable description of the  $\bar{p}$  production in  $pp$  as demonstrated above. However, to describe the AA data,  $\gamma_{qq}$  needs to be enhanced to 0.4. Using Eq. 1 this leads to an effective  $\kappa'$  of  $\kappa' = -3\pi m_q^2 / (\ln\gamma_{qq}) = 0.511$  GeV<sup>2</sup>. Thus, an increase in the string tension by a factor 2.6.

While there seems to be a strong enhancement of the antiproton production established, which causes the observed centrality dependence of the  $\bar{p}/A_{\text{part}}$  ratio, the exact cause of the enhancement remains ambiguous: several different mechanisms can lead to enhanced antiproton production: overlapping color flux tubes, QGP formation, reduced hadron masses due to partial restoration of chiral symmetry and multi-particle interactions at high densities, e.g.  $\pi\pi\pi\pi \rightarrow \bar{B}B$ . The absence of the latter type of processes in the UrQMD model (and in all other hadronic and string models, e.g. HIJING, RQMD, VENUS, etc.) leads to a violation of detailed balance. It yields significant deviations from the expected properties of an ideal hadron gas in the equilibrium limit of UrQMD (infinite volume and infinite time at fixed energy density) [24]. For the fast-changing environment and reaction dynamics of a relativistic heavy-ion collision, however, it remains open whether the inclusion of these phase-space suppressed processes would change the results significantly. On the other hand, all the above mentioned mechanisms have a strong centrality dependence and while they might be justified and used to explain the enhancement observed in the data for central collisions, their influence at peripheral impact parameters is questionable.

Further understanding of the antiproton dynamics in dense matter can be obtained by studying the anisotropic flow parameter  $v_1$  as shown in Fig. 4 for Pb(160 AGeV)+Pb interaction at impact parameters  $b \leq 11$  fm. This provides an independent and direct check of the in-medium absorption cross section. With antiproton absorption (full squares) a strong anti-flow [25] of antiprotons is predicted. The strength of the flow is 2-3 times stronger than for the proton flow (shown as full circles). If annihilation is suppressed, the anti-flow of antiprotons nearly vanishes (open squares). Thus, an experimental study of the anti-flow of antiprotons can provide direct access to the  $\bar{p}p$  annihilation cross section in dense matter.

The production and absorption of antiprotons in elementary collisions has been compared to data and reasonable agreement has been found. It has been shown that within the UrQMD model these cross sections result in an underprediction of the antiproton yield in Pb+Pb at 160 AGeV at all centralities. Suppressing of antiproton annihilation in AA collisions does

not seem to be a possible cause for the observed centrality dependence of the  $\bar{p}/A_{\text{part}}$  ratio. It is demonstrated that the measured data are consistent with an enhanced production cross section of  $\bar{p}$ 's in nucleus-nucleus collisions. The study of the anti-flow of antiprotons can give a definitive answer on the antibaryon absorption cross section in hot and dense matter.

### ACKNOWLEDGEMENTS

The authors would like to thank L. Gerland for fruitful discussions. M. Bleicher is supported by the A. v. Humboldt Foundation. S.A.B. acknowledges financial support from the U.S. National Science Foundation, grant PHY-9605207. M.Belkacem was supported by the U.S. Department of Energy under grant No. DE-FG02-87ER40328. This work is supported by the BMBF, GSI, DFG and the Graduiertenkolleg 'Theoretische und experimentelle Schwerionenphysik'. This research used resources of the National Energy Research Scientific Computing Center (NERSC).



## REFERENCES

- [1] H. Stöcker and W. Greiner, Phys. Rep. **137**, 277 (1986).
- [2] J. Harris and B. Müller, Ann. Rev. Nucl. Part. Sci. **46**, 71 (1996);  
S.A. Bass, M. Gyulassy, H. Stöcker and W. Greiner, J. Phys. **G25**, R1 (1999).
- [3] H. Stöcker, W. Greiner, W. Scheid, Z. Phys. **A286**, 121 (1978)
- [4] S. Hahn, H. Stöcker, Nucl. Phys. **A452**, 723 (1986) and Nucl. Phys **A476**, 718 (1988)
- [5] P. Koch, B. Müller, H. Stöcker, W. Greiner, Mod. Phys. Lett. **A3** (1988) 737
- [6] P. Braun-Munzinger, J. Stachel, J. P. Wessels, N. Xu, Phys. Lett. **B344**, 43 (1995);  
Phys. Lett. **B365**, 1 (1996);  
P. Braun-Munzinger and J. Stachel, Nucl. Phys. **A606**, 320 (1996).
- [7] J. Cleymans, M. I. Gorenstein, J. Stalnacke and E. Suhonen, Phys. Scripta **48**, 277 (1993).
- [8] P. Koch, B. Müller, and J. Rafelski, Phys. Rep. **142**, 167 (1986).
- [9] The CERN press release can be found at:  
<http://cern.web.cern.ch/CERN/Announcements/2000/NewStateMatter/>  
see also U. Heinz and M. Jacob, nucl-th/0002042
- [10] M. Bleicher, M. Reiter, A. Dumitru, J. Brachmann, C. Spieles, S.A. Bass, H. Stocker,  
W. Greiner, Phys. Rev. **C59** (1999) 1844 [hep-ph/9811459].
- [11] Particle Data Group, Europ. Phys. Journal **C3**, 1 (1998).
- [12] G. Cooper (NA49), Proceedings of Quark Matter '99 (Turin, Italy); Nucl. Phys. **A** in  
print
- [13] F. Sickler (NA49), Proceedings of Quark Matter '99 (Turin, Italy); Nucl. Phys. **A** in  
print

- [14] S. A. Bass et al., Prog. Part. Nucl. Phys. **41**, 225 (1998);  
M. Bleicher et al, J. Phys. G **25** (1999)
- [15] Y. Pang, D. E. Kahana, S. H. Kahana and H. Crawford, Phys. Rev. Lett. **78**, 3418 (1997) [nucl-th/9608014].
- [16] U. Heinz, P. Subramanian, H. Stöcker, W. Greiner, J. Phys. G **12** (1986) 1237
- [17] J. Ellis, U. Heinz and H. Kowalski, Phys. Lett. **B233** (1989) 223.
- [18] E. Andersen et al. (WA97 collaboration), Phys. Lett **B433**, 209 (1998).  
R. Lietava et al. (WA97 collaboration), Journal of Physics **G25**, 181 (1999).  
R. Caliendo et al. (WA97 collaboration), Journal of Physics **G25**, 171 (1999).  
S. Margetis et al. (NA49 collaboration), Journal of Physics **G25**, 189 (1999).  
F. Gabler et al. (NA49 collaboration), Journal of Physics **G25**, 199 (1999).
- [19] S. Soff, S. A. Bass, M. Bleicher, L. Bravina, E. Zabrodin, H. Stocker and W. Greiner, Phys. Lett. **B471**, 89 (1999) [nucl-th/9907026].
- [20] T. S. Biro, H. B. Nielsen, J. Knoll, Nucl. Phys. **B245**, 449 (1984). J. Knoll, Z. Phys. **C38**, 187 (1988).
- [21] H. Sorge, M. Berenguer, H. Stöcker, W. Greiner, Phys. Lett. **B289**, 6 (1992).  
N. S. Amelin, M. A. Braun, C. Pajares, Phys. Lett. **B306**, 312 (1993).  
H. Sorge, Nucl. Phys. **A630**, 522 (1998) and refs. therein.
- [22] M. Gyulassy, Quark Gluon Plasma, Advanced Series on Directions in High Energy Physics, Vol. 6, edited by R. C. Hwa, World Scientific, Singapore, 1990.
- [23] L. Gerland, C. Spieles, M. Bleicher, P. Papazoglou, J. Brachmann, A. Dumitru, H. Stöcker, W. Greiner, J. Schaffner, C. Greiner, Proc. of the 4th International Workshop, Relativistic Aspects of Nuclear Physics, Rio, Brazil, (1995), T. Kodama et al., eds., 437.

- [24] M. Belkacem, M. Brandstetter, S.A. Bass, M. Bleicher, L. Bravina, M.I. Gorenstein, J. Konopka, L. Neise, C. Spieles, S. Soff, H. Weber, H. Stöcker and W. Greiner. Phys. Rev. **C58**, 1727, (1998).
- [25] A. Jahns, C. Spieles, H. Sorge, H. Stocker and W. Greiner, Phys. Rev. Lett. **72**, 3464 (1994).

FIGURES

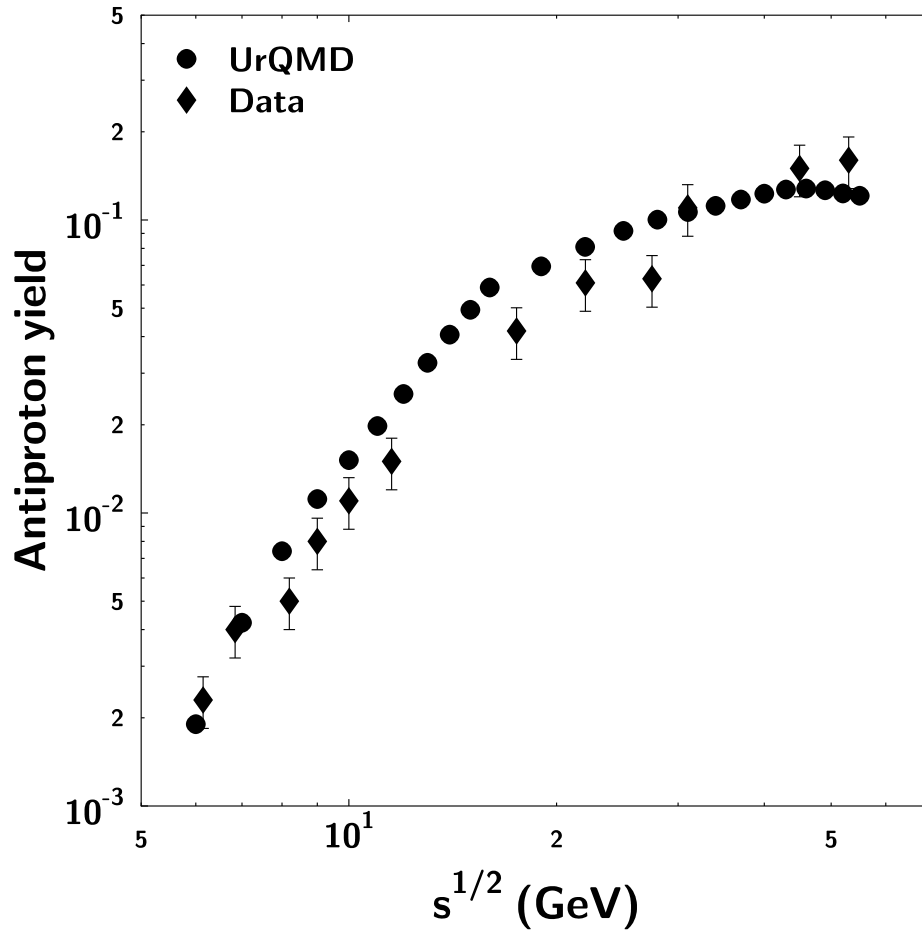


FIG. 1. Production cross sections of antiprotons in pp as a function of energy.

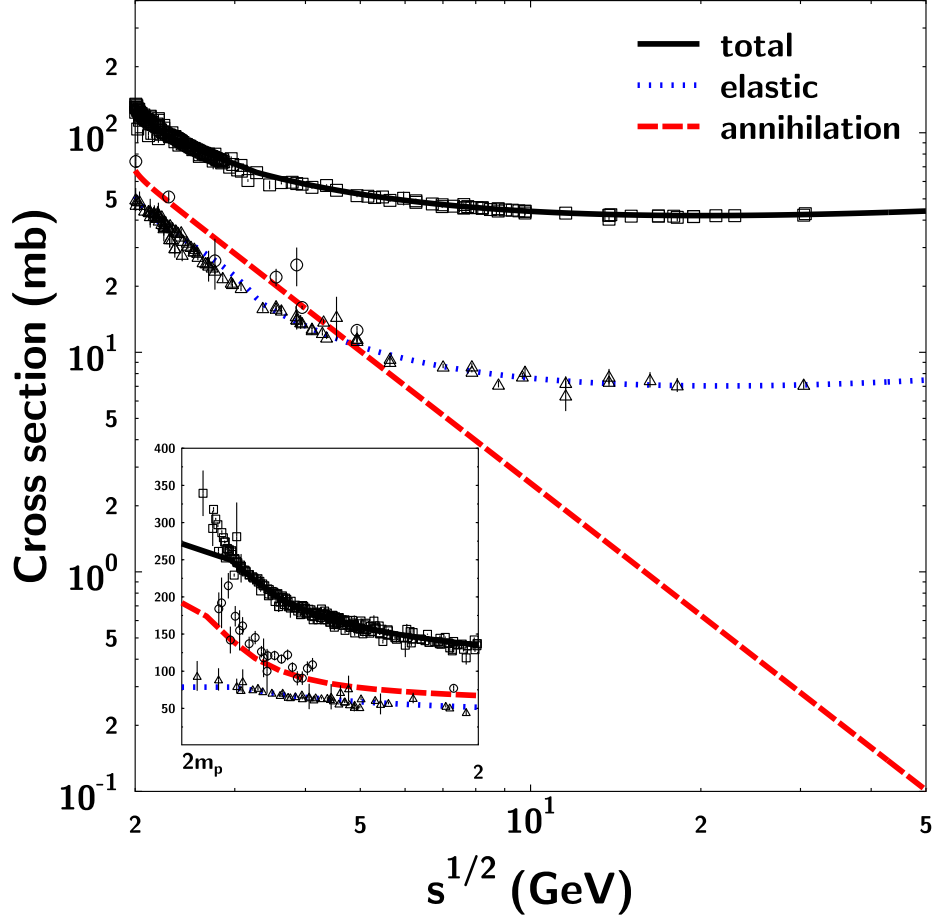


FIG. 2. Elementary antiproton-proton total, elastic and annihilation cross section as a function energy compared to data (symbols). Note that the sum of the annihilation cross section and the inelastic cross section is smaller than the total cross section. The difference  $\Delta\sigma = \sigma_{\text{total}} - \sigma_{\text{elastic}} - \sigma_{\text{annih.}}$  is assumed to be a pure inelastic cross section in  $\bar{p}p$  in analogy to  $pp$ .

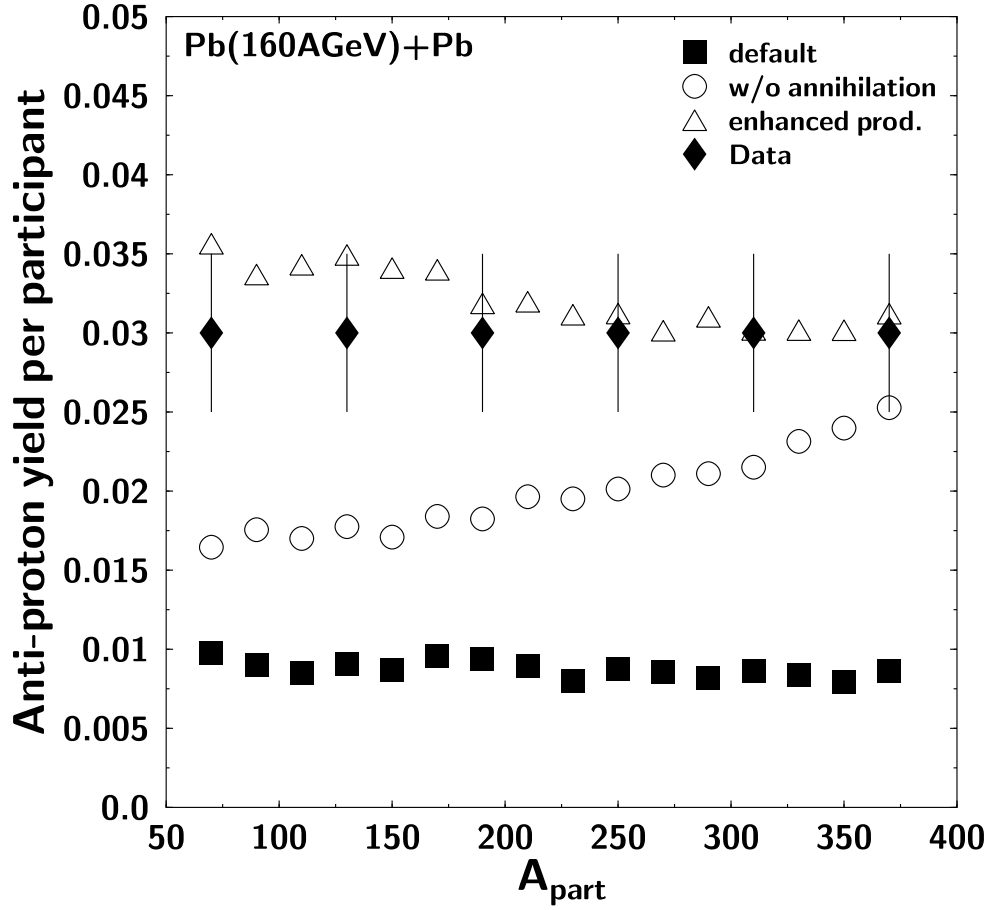


FIG. 3. Scaling of the antiprotons production with the number of participating nucleons in Pb(160 AGeV)+Pb collisions. Full diamonds depict experimental data, full squares show the standard UrQMD calculation, open circles show the UrQMD calculation with rescattering switched off, while the open triangles show UrQMD simulations with enhanced antibaryon production and standard antibaryon absorption.

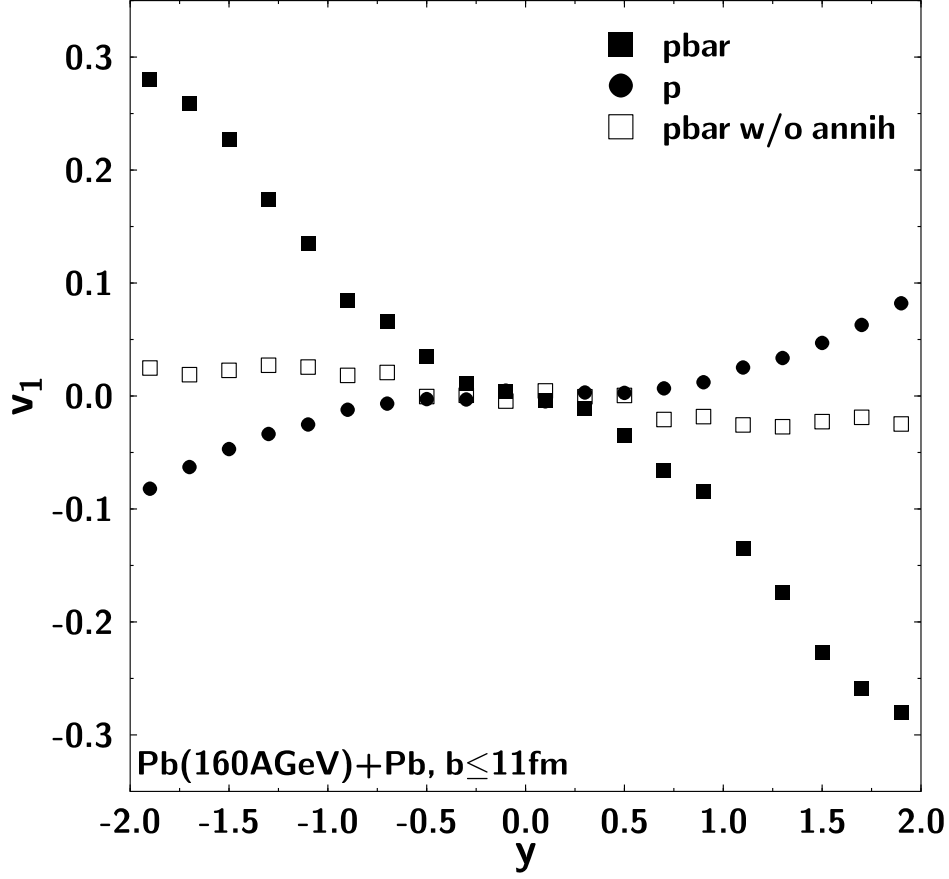


FIG. 4. Anisotropic flow parameter  $v_1$  in Pb(160 AGeV)+Pb,  $b \leq 11$  fm as a function of rapidity for protons (full circles), antiprotons (full squares) and antiprotons with annihilation switched off (open squares).